

APPLICATION OF INVERSE DESIGN METHOD TO ESTIMATION OF WIND TUNNEL MODELS

Shinkyu Jeong, Ryo Takaki and Kazuomi Yamamoto
*CFD Technology Center, National Aerospace Laboratory,
182-8522, Chofu, Tokyo, Japan*

ABSTRACT

Inverse design method is applied to geometry estimation of wind tunnel models. With the pressure distribution obtained from the wind tunnel test as the target of the inverse method, the approximate geometry estimation is carried out. The inverse method used in this paper is based on the Takanashi's concept that utilizes integral equations and 'residual-correction' technique. In this investigation, geometries of two wind tunnel models of NEXST-1 (National Experiment Supersonic Transport) were estimated. One is 23.5% scaled model and the other is 8.5%. The deviation of the inverse estimation from the original CATIA geometry was within a reasonable order if the manufacturing limitation is considered. The geometry of the 8.5% scaled model was measured for validation by using a three-dimensional non-contact measuring device employing laser beam and auto-focus system.

KEYWORDS

Inverse method, Wind tunnel models, Geometry estimation, Three-dimensional non-contact measuring

INTRODUCTION

National Aerospace Laboratory (NAL) of Japan started a scaled supersonic experimental aircraft program called NEXST [1] in 1996 to establish advanced design technologies for the next generation supersonic transport. This program is comprised of development of two types of unmanned experimental aircraft, a non-powered (NEXST-1) and a twin-jet engine airplane (NEXST-2). The main tools incorporated in the design of these aircrafts are as follow:

- 1) Carlson's method [2] for warp design
- 2) Area-Rule and Adjoint method for fuselage design [3]
- 3) Inverse method for NLF [4] (Natural Laminar Flow) wing design

A lot of wind tunnel tests and CFD analysis for NEXST configurations were conducted to predict its performance, before the flight tests.

In the 3rd SST-workshop held in Dec. 2001, many researchers supplied the CFD analysis results of NEXST-1 calculated with their own CFD-codes. These results were compared with those of wind tunnel tests. As a whole, they show a good agreement with each other. However, the pressure distributions near the 50% spanwise section, where the leading edge kink is located, show some discrepancies in the leading edge region. The pressure distribution obtained from wind tunnel test has a somewhat large peak at the leading edge region, as shown in Fig. 1.

Such a large peak at the leading edge means that transition occurs from the leading edge. As a result, NLF region will never appear on the designed wing surface.

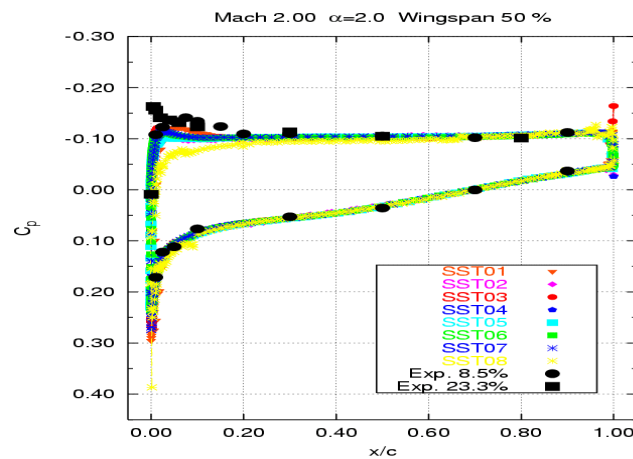


Figure 1. Pressure distributions from CFD analysis and wind tunnel tests.

Possible reasons of this discrepancy are as follows:

CFD side

1. Coarse resolution in computational grid and lack of convergence
2. Turbulence model and transition location
3. Aeroelastic deformation

Experimental side

1. Deviation from the original CATIA geometry due to limitation during manufacturing
2. Lack of experimental repeatability
3. Forced transition using roughness

In this study, the possibility of the geometric deviation of the wind tunnel model from the original CATIA geometry is investigated by solving an aerodynamic inverse problem, which is seeking a geometry yielding the prescribed pressure distribution at a given design condition. Thus if we set the pressure distribution from the wind tunnel test as the target for inverse problem, the geometry of the wind tunnel model can be estimated.

Up to date, many inverse methods are suggested for the aerodynamic design. The existing inverse methods are categorized into two groups. The first group of methods is based on the full potential flow equation. These methods solve the potential equation with the Neumann and the Dirichlet boundary condition alternately. The Neumann condition is used for flow analysis and the Dirichlet condition is for geometry correction. The methods, in this category, were developed by Carlson [5] and Tranen [6] for the airfoil design and successfully extended to three-dimensional wing design problem by Henn [7] and Shankar [8]. However, the application of these method is restricted to shock-free or weak- shock cases because of the limitation of potential flow. The second group of methods separates the geometry corrections from the flow analysis. These methods use a separated auxiliary equation for the geometry correction. Namely, the flow solver is “black-box”. Thus any type of flow analysis tool, such as the Euler solver, the Navier-Stokes solver, and even experiment can be used. These methods can be classified by the auxiliary equations they use:

- 1) The wavy-wall equations
- 2) The integral equations

The methods using the wavy-wall equation as the auxiliary equation for the geometry correction were developed by Warren [9] and improved by Malone [10] and Santos [11]. This method was

successfully adapted to the two-dimensional airfoil design. However, the application to the three-dimensional wing design problem shows some limitation because the formulation of the auxiliary equation is basically two-dimension. On the other hand, the integral equation approach [12] is formulated in three-dimension. This method was developed by Takanashi and was successfully applied to three-dimensional transonic wing design.

In this study, the inverse method using integral equations was applied to the approximate estimation of the wind tunnel model. Two differently scaled NEXST-1's wind tunnel models were used for validation. One is 23.5% scaled model, which is intended for transition characteristics measurement, and the other is 8.5% scaled model, for force and pressure measurement. In the case of 8.5% scale wind tunnel model, the three-dimensional non-contact geometry measurement was also conducted. The geometry of original CATIA data, inverse estimation, and three-dimensional measurement were compared. Furthermore, CFD analysis was also performed for the measured-geometry.

INVERSE METHOD

The procedure of the present inverse method is shown in Fig.2.

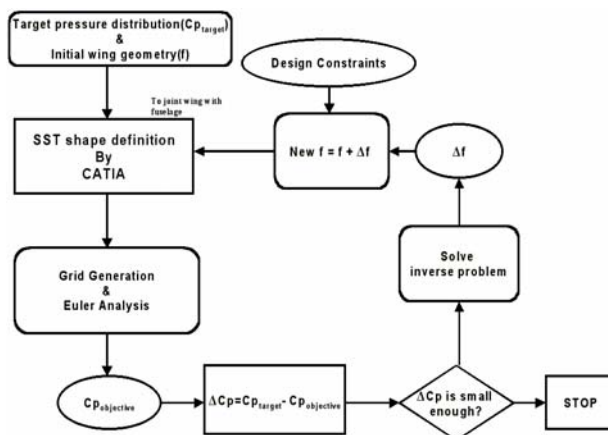


Figure 2. Flow-chart of the inverse method.

- 1) Arbitrary initial wing geometry and the target pressure distribution are input.
- 2) Flow analysis around the initial wing geometry is performed, and the difference between the objective and the target pressure distribution is calculated.
- 3) From this difference, the geometry correction is determined by solving integral equations.
- 4) Adding the geometry correction to the initial wing geometry, new wing geometry is obtained.
- 5) Routines 2)~4) are iterated until the difference between objective and target pressure distribution becomes small enough.

The original Takanashi's method is for subsonic and transonic flow. The extension to supersonic flow region was carried out by the author. The integral equations for supersonic flow [13] are as follow: The integral equation for thickness correction

$$\Delta u_s(x, y) = -\Delta w_s(x, y) + \frac{1}{\pi} \iint_{\Sigma_1} \frac{(x-\xi)\Delta w_s(\xi, \eta)}{\sqrt{(x-\xi)^2 - (y-\eta)^2}} d\xi d\eta \quad (1)$$

$$\Delta u_s(x, y) = \Delta \phi_x(x, y, +0) + \Delta \phi_x(x, y, -0) \quad (2)$$

$$\Delta w_s(x, y) = \Delta \phi_z(x, y, +0) - \Delta \phi_z(x, y, -0) \quad (3)$$

The integral equation for camber correction

$$\Delta w_a(x, y) = -\Delta u_a(x, y) + \frac{1}{\pi} \iint_{\tau_1} \frac{(x-\xi)\Delta u_a(\xi, \eta)}{(y-\eta)^2 \sqrt{(x-\xi)^2 - (y-\eta)^2}} d\xi d\eta \quad (4)$$

$$\Delta u_a(x, y) = \Delta \phi_x(x, y, +0) - \Delta \phi_x(x, y, -0) \quad (5)$$

$$\Delta w_a(x, y) = \Delta \phi_z(x, y, +0) + \Delta \phi_z(x, y, -0) \quad (6)$$

The symbol Δ indicates the difference between target and objective. $\Delta \phi_x$ and $\Delta \phi_z$ can be represented as follows:

$$\Delta \phi_x(x, y, \pm 0) = -\frac{1}{2} \Delta C_{p\pm}(x, y) \quad (7)$$

$$\Delta \phi_z(x, y, \pm 0) = \frac{1}{\beta^3} \frac{\partial \Delta f_{\pm}(x, y)}{\partial x} \quad (8)$$

where the subscript ' \pm ' denotes the upper and lower surface of the wing, respectively. ($\beta^2 = M^2 - 1$) The integrated value for thickness correction, however, does not always satisfy closure condition at trailing edge. To settle this problem, Δw_s is modified as follows:

$$\Delta w_s^{\text{mod}}(x, y) = \Delta w_s(x, y) - \frac{\int_{L.E.}^{T.E.} \Delta w_s(\xi, y) d\xi}{l} \quad (9)$$

$$\int_{L.E.}^{T.E.} \Delta w_s^{\text{mod}}(\xi, y) d\xi = 0 \quad (10)$$

where l is local chord length at each spanwise location.

The geometry correction can be computed by performing the numerical integration in the x-direction.

$$\Delta z_{\pm}(x, y) = \frac{1}{2} \int_{L.E.}^x \Delta w_a(\xi, y) d\xi \pm \frac{1}{2} \int_{L.E.}^x \Delta w_s^{\text{mod}}(\xi, y) d\xi \quad (11)$$

RESULTS

The verification of the present inverse estimation method was performed with the NEXST-1's wind tunnel models mentioned above. The target pressure distribution used for the inverse estimation is defined using the pressure data from wind tunnel test. However, the number of the pressure data from the wind tunnel test is not enough for the inverse estimation. The 6th spline function is used for interpolation of the pressure data. The interpolated target pressure distribution is shown in fig. 3.

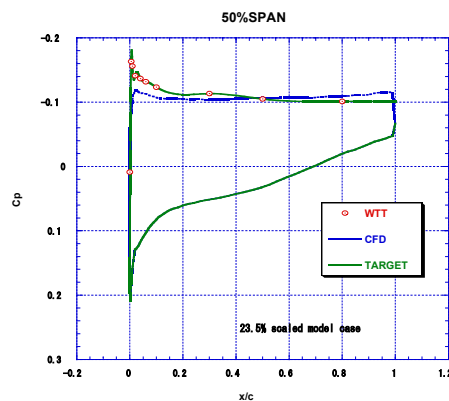


Figure 3. The interpolated target pressure distribution for inverse estimation

Case1: 23.5% model

In the case of 23.5% cased model, the largest discrepancy between pressure distribution from CFD analysis and that from wind tunnel test was located at 50% spanwise section. The discrepancies in spanwise regions less than 30% and more than 70% were negligible compared to that of 50% spanwise section as shown in Fig 4.

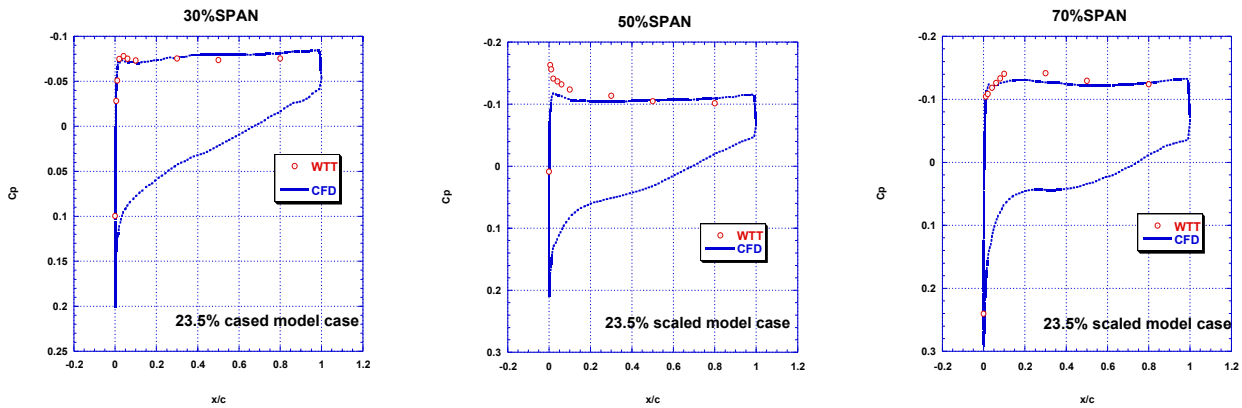
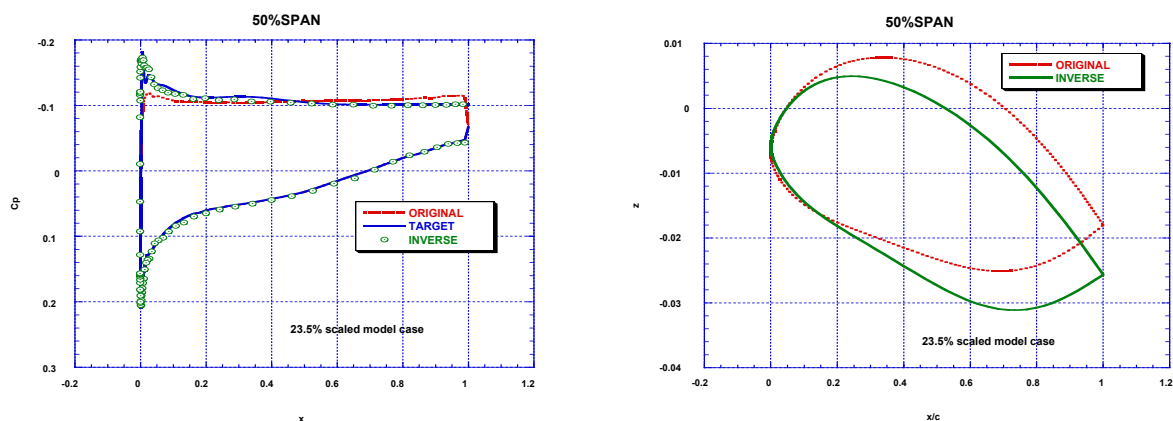


Figure 4. Comparison of pressure distributions between wind tunnel test data and CFD data.

Thus, in the 23.5% cased model case, the target pressure distribution for the inverse estimation was defined as follows:

- In spanwise regions less than 30% and more than 70%: The pressure distribution from CFD analysis is set to be equal to the target pressure distribution
- In spanwise region between 30% and 70%: Using the pressure distributions at 30%, 50% and 70% spanwise sections obtained from wind tunnel test, the pressure distributions are interpolated linearly.

Figure 5a) compares the target pressure distributions, that of original geometry, and that of the geometry obtained by the inverse estimation after 4 iterations. The inverse estimation approached the target very closely. Figure 5b) shows the corresponding geometries. The maximum thickness deviation at leading edge region is about 0.4mm, which is 0.094% decrease compared with the original geometry.



(a) Pressure distributions

(b) Geometries

Figure 5. Comparison of pressure distributions and corresponding geometries.

The shape of the estimated geometry is largely different from that of the original one. The reason of this large difference may be a non-uniqueness of the present inverse method [14]. The present inverse method has the possibility of having many geometry solutions for the specified pressure distribution. In order to obtain the geometry that satisfies our purpose, geometry constraints should be imposed.

Case 2: 8.5% model

In contrast to the 23.5% scaled model, the discrepancy of pressure distributions from the wind tunnel test and CFD analysis at spanwise sections other than 50% is not negligible, as shown in Fig. 6.

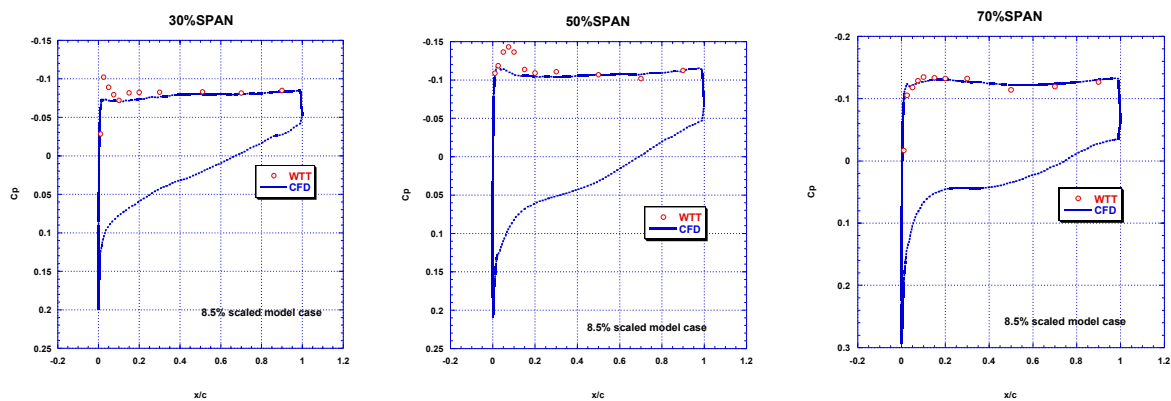
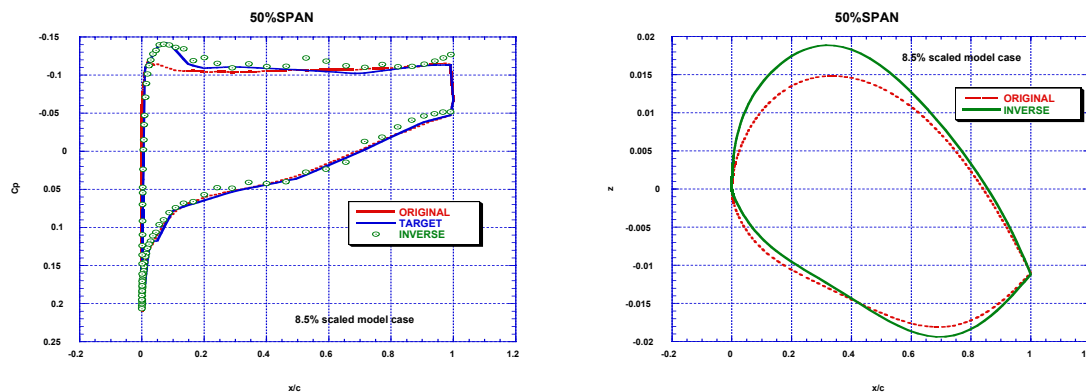


Figure 6. Comparison of pressure distributions between wind tunnel test data and CFD data.

Thus, here the target pressure distribution of the inverse estimation was defined as follows:

- In spanwise regions less than 12% and more than 90%: The pressure distribution from CFD analysis is set to be equal to the target pressure distribution.
- In spanwise region between 12% and 90%: Using the pressure distributions at 12%, 30%, 50%, 70% and 90% spanwise sections obtained from wind tunnel test, the pressure distributions are interpolated linearly.

The inverse geometry estimation of the 8.5% scaled model was performed with the fixed leading- and trailing-edge constraint under the assumption that the edges are accurately manufactured. Figure 7a) compares the target pressure distribution, that of the original geometry, and that of the geometry obtained from the inverse estimation at 50% spanwise section. After 6 inverse iterations, the pressure distribution of the geometry obtained from the inverse estimation almost converged to that of target. The corresponding geometry is shown in Fig. 7b). The maximum thickness deviation at leading edge region is about 0.3mm, which is 0.18% increase compared to the original geometry.



(a) Pressure distributions

(b) Geometries

Figure 7. Corresponding geometry of CFD analysis and obtained by inverse method.

Three-dimensional non-contact measuring

The geometry deviation of the inverse estimation is in the order of 0.1mm. For verification, the 8.5% scaled wind tunnel model was measured with a three-dimensional non-contact measuring device, as shown in Fig. 8. The device employs a laser beam and an auto-focus system. With this device, which has a resolution of $0.1 \mu\text{m}$, the geometry of wind tunnel model can be measured more accurately than with contact measurement device.

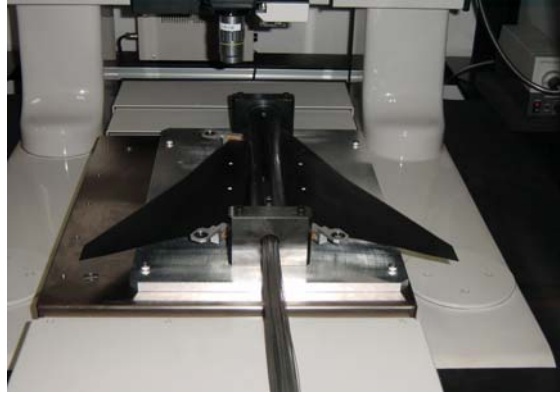


Figure. 8 Three dimensional non-contact measuring device

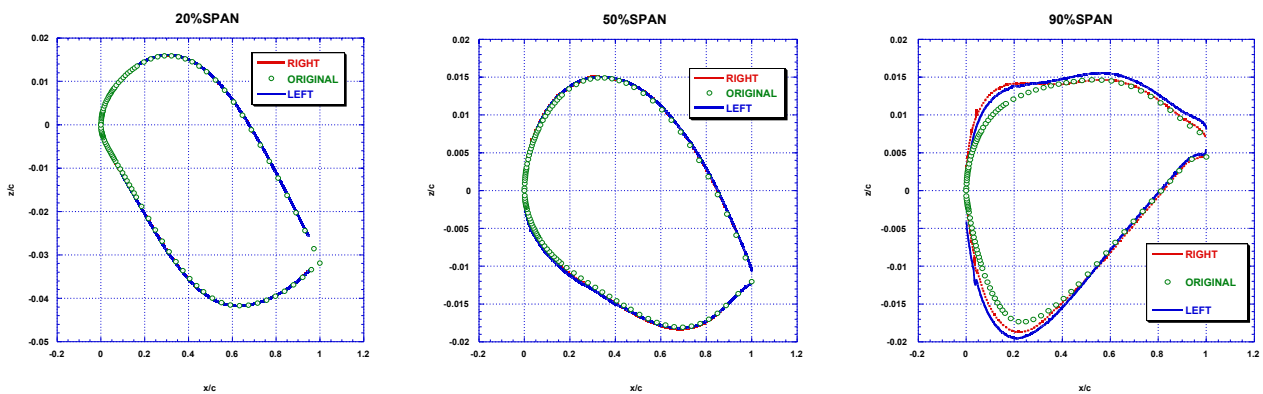
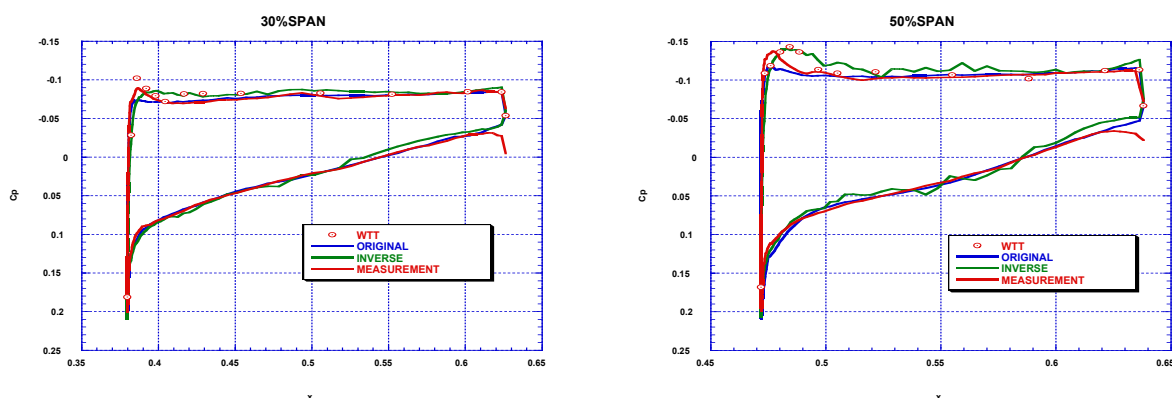


Figure 9. Measurement results

Measurement results are shown in Fig. 9. It shows a good agreement with the original CATIA geometry in inboard region. The maximum thickness deviation near the leading edge at 50% spanwise sections is about 0.15mm, an increase of 0.09% compared to the original CATIA geometry. About 0.1 mm's deviation is reasonable, considering the limitation of manufacturing. However, in outboard region, the discrepancy is very large.

The CFD analysis around the measured-geometry is also performed. The results are shown in Fig 10.



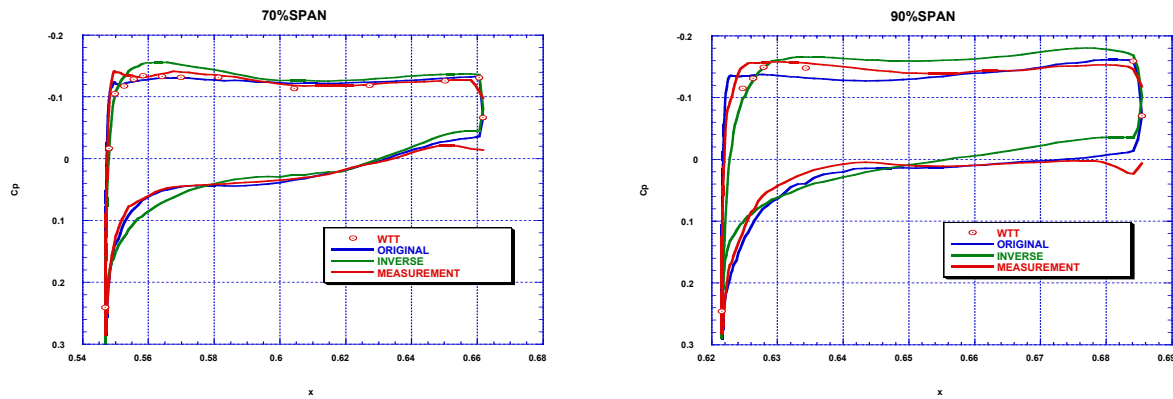


Figure. 10 Comparison of pressure distribution among WTT, original, inverse and measurement geometry

CONCLUDING REMARK

In this study, the inverse method is applied to investigate the deviation of the wind tunnel model from the original geometry. By defining the pressure distribution obtained from wind tunnel test as the target of the inverse method, approximate geometry estimation was carried out. The geometry of two wind tunnel models of NEXST-1 were estimated, one was the 23.5% scaled model and the other was the 8.5%. In the case of 8.5% scaled wind tunnel model, the geometry was measured with a three-dimensional measuring device. In this case, the inverse estimation predicted that the maximum geometry deviation at the 50% spanwise section is about 0.3mm. However, the measurement result shows that the deviation from the original CATIA geometry at the 50% spanwise section is about 0.15 mm. The inverse method cannot predict the geometry of the wind tunnel models accurately, even though the pressure distribution is very close to that of target. This is probably due to the non-uniqueness of the inverse problem. Adequate geometry constraint should be imposed on the inverse method for accurate geometry estimation of wind tunnel model.

From the results of the investigation, the prescribed difference of NEXST-1's pressure distributions between the CFD analysis and the wind tunnel test is probably not conclude to the deviation of the wind tunnel model. Other reasons should be investigated, especially in the CFD side. The NEXST-1 is designed to obtain natural laminar flow (NLF) on the wing surface, which requires a very stiff suction peak at its leading edge followed by very slow acceleration region. However, this kind of pressure distribution is very sensitive even to small perturbation, and is difficult to maintain. Furthermore, the flow can easily separate. In order to predict this kind of flow accurately with CFD, one must pay great attention to issues such as grid resolution, turbulence model, and transition prediction.

REFERENCES

1. K. Sakata, "Supersonic Experimental Airplane Program in NAL (NEXST) and its CFD-Design Research Demand," 2nd International Workshop on CFD fort SST, pp. 53-56, Jan., 2000.
2. H. W. Carlson and W. D. Middleton, "A Numerical Method for the Design of Camber Surface of Supersonic Wings with Arbitrary Planform," NASA TN D-2341, 1964.
3. Y. Makino, T. Iwamiya and Z. Lei, "Fuselage Shape Optimization of Wing-body Configuration

- with Nacelles,” AIAA 2001-2447, 2001.
4. K. Matsushima, T. Iwamiya and W. Zhang, “Inverse Wing Design for Scaled Supersonic Experimental Airplane with Ensuring Design Constraints,” 2nd International Workshop on CFD for SST, pp. 91-96, 2000
 5. L. A. Carlson, “Transonic Airfoil Design Using Cartesian Coordinates,” NASA CR-2578, 1976.
 6. T. L. Tranen, “A Rapid Computer Aided Transonic Airfoil Design Methods,” AIAA Paper 74-501, 1974.
 7. P. A. Henne, “Inverse Transonic Wing Design Method,” *Journal of Aircraft*, Vol. 18, No. 2, pp. 121-127, February 1981.
 8. V. Shankar, “A Full Potential Inverse Method Based on a Density Linearization Scheme for Wing Design,” AIAA Paper 81-1234, 1981.
 9. W. H. Davis, Jr., “Technique for Developing Design Tools from the Analysis Methods of Computational Aerodynamics,” *AIAA Journal*, Vol. 18, No. 9, pp. 1080-1087, September 1980.
 10. J. B. Malone, J. Vadyak and L. N. Shankar, “A Technique for the Inverse Aerodynamic Design of Nacelles and Wing Configurations,” AIAA Paper 85-4096, 1985.
 11. L. C. Santos and L. N. Sankar, “A Hybrid Inverse Optimization Method for the Aerodynamic Design of Lifting Surfaces,” AIAA Paper 94-1895, 1994.
 12. S. Takanashi, “Iterative Three-Dimensional Transonic Wing Design Using Integral Equations,” *Journal of Aircraft*, Vol. 22, No. 8, pp. 655-660, August 1985.
 13. S. Jeong, S. Obayashi, K. Nakahashi, K. Matsushima and T. Iwamiya, “Iterative Design Method for Supersonic Wings Using Integral Equations,” *Computational Fluid Dynamics Journal*, Vol. 7, No. 3, pp. 356- 374, October, 1998.
 14. S. Jeong, S. Obayashi and K. Nakahashi, “Supersonic Inverse Design method with Twist Specification,” the proceedings of 16th International Conference on Numerical Method in Fluid Dynamics, pp. 263-264, France, July, 1988.